

# Study and design of a coaxial magnetic gear with a high torque density in telescopic camera cranes

Piotr WARMUZEK<sup>ib</sup>, Janusz KOŁODZIEJ<sup>ib\*</sup>, and Marcin KOWOL<sup>ib</sup>

Opole University of Technology, Faculty of Electrical Engineering, Automatic Control and Informatics, Opole, Poland

**Abstract.** Magnetic gears are slowly becoming a natural alternative to mechanical gears. Providing contactless, frictionless, and low-noise torque conversion, they are finding applications in renewable energy sources and electric vehicles, among others. This paper presents a comprehensive theoretical analysis with numerical calculations of a magnetic gear (MG) design for novel applications in telescopic camera cranes. Based on numerical simulations of selected MG variants, a potential transducer configuration was chosen that would meet the requirements of the drive transmission system – supporting the movement of the telescopic camera crane arm.

**Keywords:** telescopic camera cranes; magnetic gear; magnetic torque; torque ripple; radial forces.

## 1. INTRODUCTION

Magnetic gears are relatively new transducers that have been intensively researched and developed over the last two decades. Although the concept of building magnetic gears dates back to the beginning of the 20th century, the development of these transducers was initially slow due to material limitations, which determined/resulted in relatively low values of transmitted torques. Additionally, the first magnetic gears were built as equivalents of mechanical gears, in which the teeth were replaced with interacting magnets [1, 2]. Only a tiny percentage of magnets simultaneously participate in energy transformation in such structures, significantly limiting the range of loads supported. These structures, mainly due to the low density of transmitted torque, lost in competition with constantly developed mechanical transmissions and were not used in industry. The invention of high-energy permanent magnets, manufactured based on rare earth elements, significantly influenced the development of the design of electromechanical transducers and also significantly increased the efficiency of magnetic transmissions. However, only the new design solution proposed by Atallah [3] in the form of a concentric magnetic gear with a modulator – ferromagnetic poles modulating the rotors' magnetic fields – caused a breakthrough. Magnetic gears have become an attractive alternative to mechanical gears, especially in wind energy, transforming the mechanical energy of a low-speed turbine to the needs of a high-speed generator. Replacing geared mechanical transmissions that suffer from increased noise levels, vibrations, and the need for servicing significantly reduces the risk of costly wind turbine failures [2, 4]. Magnetic gears have been intensively developed in recent years; structures with axial and radial

magnetic flux, Hallbach magnetization in rotors, harmonic and cycloidal gears, etc., have been created [1, 2, 5–7]. The development of magnetic gears will reduce the costs of servicing and repairing mechanical gears, limiting failures. The lack of physical contact protects against overloads and provides the separation required in some applications. So far, the research has focused mainly on effective modeling techniques for these transducers, such as increasing torque density and reducing pulsation, as well as aspects related to practical application and assembly. Currently, proposed structures are characterized by torque densities exceeding  $200 \text{ kN}\cdot\text{m}/\text{m}^3$ , but most of these structures transfer relatively small torques of 100–200 N·m. Few publications in the literature describe transducers operating at torques of the order of kN·m, and there are even fewer works containing test results confirmed by measurement on prototypes [7–11]. The paper aims to check whether using a coaxial magnetic gear to assist the rotation of a telescopic camera crane is possible (Fig. 1). The authors of the work analyze possible solutions for a single-stage radial MG, looking for a structure that meets very high requirements regarding the quality of the drive system operation. The research covers, in particular, the value and shape of the torque wave, stress analysis in local and overall terms, and indicates the final design solution that can be applied.



Fig. 1. Telescopic camera crane

\*e-mail: ja.kolodziej@po.edu.pl

Manuscript submitted 2024-09-02, revised 2025-01-16, initially accepted for publication 2025-03-13, published in July 2025.

## 2. BASIC ASSUMPTIONS OF THE CAMERA CRANE SUPPORT SYSTEM

The advantages of magnetic gears, such as low noise and vibration levels, minimal failure rate, no need for lubrication and servicing, and resistance to overload, are desirable in telescopic cranes for cameras. The devices are critical to the niche film and television production equipment industry but receive little attention in the scientific literature. The first camera cranes invented in the 1980s were constantly developed, and currently, cranes with lengths from 3 m to 23 m are on the market. These are devices moved by the power of human muscles, and the largest of them is characterized by high inertia resulting from the arm's mass reaching up to 3 t. Operating such devices requires a lot of skill and experience, and inappropriate movement of the telescopic arm may, due to high inertia, be dangerous for people and the devices themselves. Developing a system containing a magnetic gear that assists the movement of the telescopic camera crane arm in two axes is an interesting issue that will significantly improve the ergonomics and safety of using these devices. Due to the application area, telescopic camera cranes are subject to high requirements for low noise emissions, vibrations, and failure-free operation.

The purpose of the camera crane movement assist system is to reduce the forces significantly applied to the arm handles. It was assumed that reducing the forces by 50% would be sufficient support to move the arm comfortably. The average value of maximum torque and rotational speed required at the gear output was obtained based on a series of measurements during the regular boom operation. Following the assumptions of the movement assist system, the MG must transmit a torque of 0.8 kN·m at a speed of 5 rpm. The critical assumption of the designed drive system is quiet operation. The gear is designed to work mainly with a low-speed, high-torque motor to reduce noise emission. However, additional limitations are the installation space and the power source's available power. To reduce the transducer's volume (and thus increase its torque density), a design is sought that places the motor inside the magnetic gear. The preselected 4 kW torque motor, which meets power supply limitations and dimensional constraints, has a torque of 90 N·m and a maximal speed of about 400 rpm. This selected configuration determines the minimum internal diameter of the gear. The available mounting space in existing boom designs also defines the transducer's outer diameter and active length. The MG design must also be scalable, so an adjustable segmented system is preferred. The critical constant parameters of the gear are included in Table 1. In the next part of the work, the authors will analyze several gear design solutions under the adopted assumptions, searching for the potentially best transducer.

**Table 1**  
Magnetic gear requirements

Parameter	Value
Inner diameter	240 mm
Outer diameter	330 mm
Active length	100 mm
Minimal torque for the output rotor	800 N·m

## 3. NUMERICAL MODEL AND CALCULATION OF THE MAGNETIC GEAR

The principle of operation of a coaxial magnetic gear requires ensuring an appropriate combination of the number of rotor pole pairs and modulator pole pieces ( $n_s$ ) [12]. Assuming that the inner rotor ( $p_i$ ) is driven and the outer rotor ( $p_o$ ) is planned as the output, the MG ratio can be calculated from the ratio  $i_r = p_o/p_i$ , but at the same time, the condition regarding the number of modulator poles  $n_s = p_o + p_i$  must be met.

The critical aspects of MG design and modeling are widely described in world literature. The authors devote much attention to the modulator, its shape, and the materials used for its construction to determine the quality of MG [13]. All models included in this work use a modulator in the form of a stack of sheets with internal magnetic bridges. The outer and inner diameters of the modulator were selected to maintain a 1 mm thickness of air gaps. Both MG rotors were modeled as packaged sheet metal yokes using permanent magnets (N42) with radial magnetization and surface mounting. The thickness of the magnets was selected based on the authors' experience. To limit the search space in addition to the geometric limitations contained in Table 1, transducers with the number of modulator pole pieces in the range of 31–36 were analyzed in the parameterized numerical model. The generated example two-dimensional MG model is shown in Fig. 2.

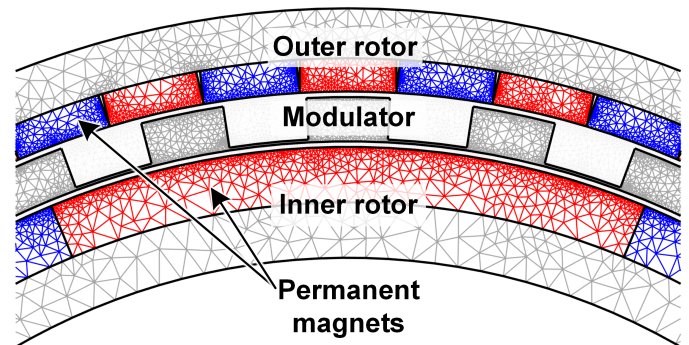


**Fig. 2.** Part of the numerical model of the magnetic gear

The radial force component between the gear rotors is an important factor influencing the radial tensions that increase the MG noise levels. The occurrence of radial forces is closely related to the magnetic symmetry of the gear ( $x_s$ ) and directly depends on the number of rotor pole pairs and modulator poles. According to [14, 15], radial forces do not occur when there is a relationship between the number of pole pairs of the inner rotor and the modulator poles:

$$x_s = gcd(2p_i, n_s) \geq 2, \quad (1)$$

where  $x_s$  is the symmetry coefficient,  $gcd(a, b)$  is the greatest common divisor of numbers  $a$  and  $b$ .

As the number of pole pairs of the low-speed (outer) rotor is also related to the number of modulator pole pieces through the gear ratio, the fulfillment of relation (1) is sufficient for the entire MG. Local tensions in transducers with magnets are a natural

phenomenon; they must cancel each other globally. The symmetry coefficient  $x_s$  informs about the occurrence of unbalance in a given MG, but numerical calculations are necessary to assess the force value. The calculation results presented in Table 2 include 24 MG variants, their respective values of the  $x_s$  coefficient, and the maximum tensions for both rotors in the least favorable operating condition – with the external rotor blocked. In the extreme case, for the M12 variant, the tension reaches over 2.7 kN. Analyzing the data in Table 2, it is also visible that the forces are close to zero when the symmetry condition is met.

Eliminating radial tensions is a critical issue in the design of MG [16]. Due to the principle of operation of the field-modulated magnetic gear (FMMG), the presence of a modulator determines the degree of coupling of the appropriate harmonics, depending on the combination of the number of rotor pole pairs, which translates into the value of the magnetic torque. The calculation results included in Table 3 illustrate the maximum torque values obtained by individual MG variants. Half of the analyzed variants meet the assumed torque criterion (0.8 kN·m), but it is also necessary to investigate the shape of the torque wave – possible torque ripple. Magnetic symmetry may result in torque ripple and cogging torque, which may cause difficulties in controlling the drive and vibration of the device and increase

noise emissions. It was noticed that the  $x_s$  coefficient is equal to the  $C_t$  coefficient, determining the severity of cogging torque [17]. The slightest torque ripple was observed for the coefficient  $C_t = x_s = 1$ , but this value results in radial forces in the gear. The coefficient  $\varepsilon$  determines the torque ripple value (2):

$$\varepsilon = (T_{\max} - T_{\min}) / (2 \cdot T_{av}), \quad (2)$$

where  $\varepsilon$  is the torque ripple value,  $T_{\max}$ ,  $T_{\min}$ ,  $T_{av}$  – maximum, minimum, average torque respectively.

The element most exposed to torque ripple is the driven (internal) rotor. The level of torque ripple is related to the gear ratio value and generally decreases with its decrease, but it also depends on the value of the symmetry coefficient. Considering a compromise between the value of the transferred torque, the exclusion of radial forces, and torque ripple, four variants were selected for further consideration: M7, M11, M15, and M19. The static characteristics of the magnetic torque for the mentioned structures are shown in Fig. 3. All variants are characterized by a torque value adequate to the requirements. Due to the lack of magnetic symmetry, only the M19 variant has negligibly small pulsations but at the expense of radial forces. A relatively high torque ripple coefficient characterizes the three variants with no

**Table 2**

Magnetic gear variants and calculated maximal force

Model	$p_i$	$n_s$	$p_o$	$i_r$	$gcd$	$F_{in}$ [N]	$F_{out}$ [N]
M1	1	31	30	30k	1	654.7	249.7
M2	2	31	29	14.50	1	345.7	155.7
M3	3	31	28	9.33	1	2219.5	959.1
M4	4	31	27	6.75	1	599.2	389k
M5	1	32	31	31k	2	1.73	3.07
M6	2	32	30	15k	4	2.37	4.3
M7	3	32	29	9.67	2	2.69	5.95
M8	4	32	28	7k	8	6.52	5.58
M9	1	33	32	32k	1	615.39	198.4
M10	2	33	31	15.50	1	1359.4	485.7
M11	3	33	30	10k	3	4.15	14.9
M12	4	33	29	7.25	1	2710.1	1120k
M13	1	34	33	33k	2	1.59	6.04
M14	2	34	32	16k	2	2.24	3.13
M15	3	34	31	10.33	2	2.44	3.5
M16	4	34	30	7.50	2	2.93	8.52
M17	1	35	34	34k	1	580.9	159.1
M18	2	35	33	16.50	1	283.7	92.8
M19	3	35	32	10.67	1	322.7	138.9
M20	4	35	31	7.75	1	197.3	27.6
M21	1	36	35	35k	2	2.2	10.3
M22	2	36	34	17k	4	2.88	7.71
M23	3	36	33	11k	6	4.97	8.74
M24	4	36	32	8k	4	5.78	5.47

**Table 3**

Calculated magnetic torque and torque ripple

Model	$T_{in}$ [N·m]	$T_{out}$ [N·m]	$\varepsilon_{in}$ [%]	$\varepsilon_{out}$ [%]
M1	24.58	305.4	131.4	0.31
M2	43.95	561.9	13.3	0.08
M3	85.03	772.4	2.67	0.07
M4	140.6	943.3	0.7	0.06
M5	77.18	313.2	624.2	2.86
M6	174.1	580.9	330.3	3.58
M7	93.42	778.4	15.85	0.11
M8	403.6	1006.4	175.6	6.81
M9	22.77	306.7	129.8	0.31
M10	41.33	568.5	12.5	0.08
M11	118.3	786.4	47.49	0.24
M12	133.4	960.6	0.7	0.05
M13	72.37	312.5	627.9	2.44
M14	61.05	571.3	67.04	0.27
M15	87.77	790.1	14.7	0.06
M16	137.7	970.4	6.45	0.10
M17	21.2	306.6	128.9	0.24
M18	38.69	571.6	11.72	0.11
M19	76.09	793.3	2.27	0.08
M20	126.6	976.1	0.66	0.06
M21	68.02	312.1	633.1	2.29
M22	152.9	584.4	329.1	2.71
M23	248.6	808.3	229.1	3.74
M24	170.1	982.6	36.63	0.32

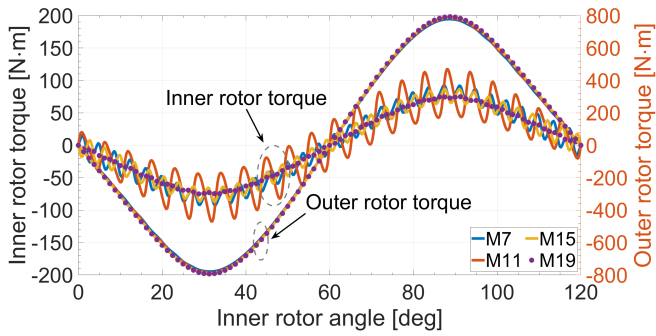


Fig. 3. Torque calculations for the selected variants

radial forces. According to the literature, magnetic symmetry causes pulsations, and one of the methods to eliminate them is skewing. The most promising M15 variant was selected for further consideration and, after detailed analysis, can be further optimized in terms of dimensions to best suit the requirements of the camera crane support system.

#### 4. ANALYSIS OF SELECTED MODELS

One of the most effective methods of reducing torque ripple in electrical machines is to reduce the cogging torque by skewing the stator slots or permanent magnets on the rotor. Arranging the magnets in a segmented diagonal skew along the shaft axis, with a specific angular shift – discrete skewing, is a frequently used procedure for surface mounting of rotor permanent magnets. This procedure can also be performed in magnetic gears, but it is crucial to determine the value of the skewing angle.

A detailed analysis of this issue is included in the work [17], where the authors provide analytical relationships determining the skew angle eliminating selected harmonics based on the harmonic spectrum. In the MG (M15) model, the gear ratio is fractional (10.33), the  $x_s = 2$ , there are no radial tensions, and the problem mainly concerns the torque ripple on the internal rotor –14.7% (blue line in Fig. 4). The dominant harmonic for the inner rotor can also be calculated using equation (3):

$$k = lcm(2p_i, n_s) \quad (3)$$

and for the selected variant, it is 102. Accordingly, the required skew angle can be calculated as  $\alpha_s = 360^\circ / 102 = 3.52^\circ$ . As seen in Fig. 4, when using five layers, the torque ripple problem was

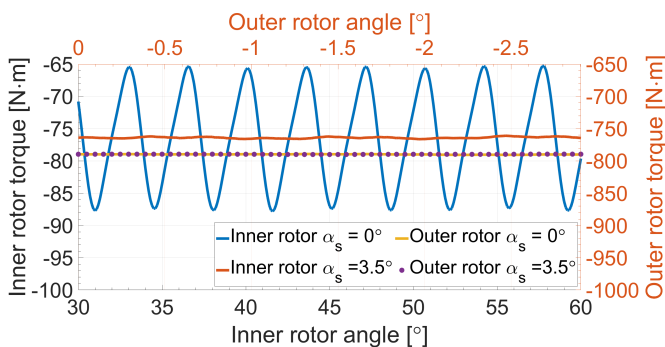


Fig. 4. Magnetic torque for maximum load for the M15 model

solved – the  $\varepsilon$  coefficient value is 0.84%. More importantly, no significant change/decrease in the average torque value was observed.

MG second potentially attractive design solution is the M19 model (Fig. 5), characterized by a low torque ripple of about 2.27% on the internal rotor. However, it suffers from relatively high radial forces on both rotors ( $F_{in} > 300$  N). Analyzing the FFT spectrum of the forces distribution, one can see the relationship between the harmonic forces acting on the rotors and the number of modulator pole pieces. Figure 6 shows the variability of the force components before and after applying the skewing for both rotors for a rotation angle equal to the polar pitch of the modulator. The resultant radial tension concerning the internal rotor has been reduced more than ten times to approximately 20 N.

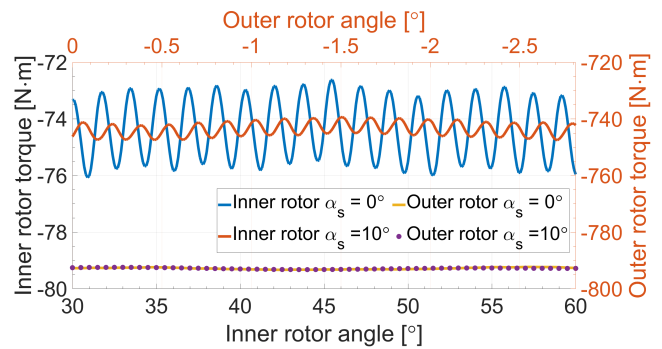


Fig. 5. Magnetic torque for maximum load for the M19 model

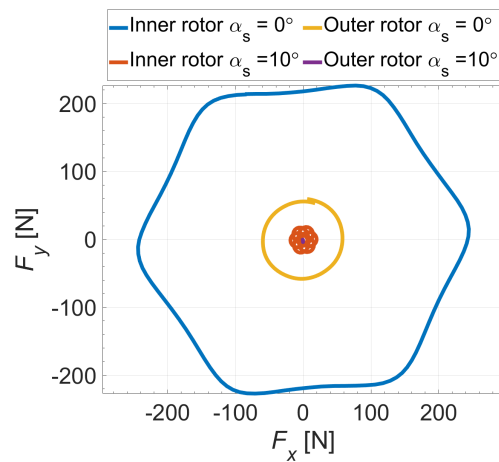


Fig. 6. Variation of force components for the M19 model

#### 5. CONCLUSIONS

Considering the relationship between the number of magnetic poles of rotors and modulator pole pieces (see Section 3), the choice of MG configuration is seemingly arbitrary. Only a few of the 24 configurations analyzed in this work have application potential. The obstacles are radial tensions and torque pulsations occurring in most MG variants. As shown later in the work, there are effective methods of reducing these unfavorable phenomena.

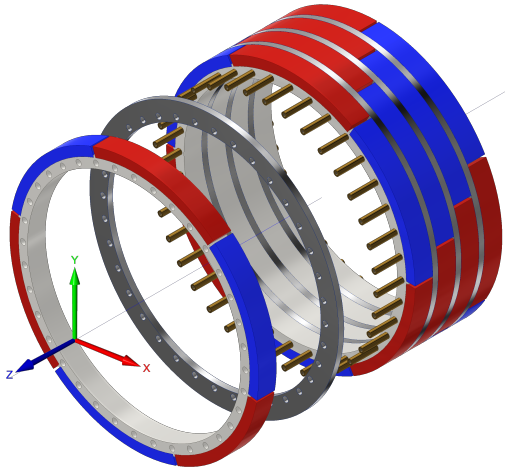


Fig. 7. Structure of the inner rotor with a skewed magnet

Applying a skew of the high-speed rotor to the M15 and M19 solutions selected after initial analysis eliminates the harmful features. In the authors' intention, the skew concerning the internal rotor can be implemented using a segmented structure (Fig. 7). Segmentation of magnetic poles should facilitate assembly and reduce prototype production costs. It is also beneficial due to the reduction of eddy current losses. The two-dimensional calculations presented in this work generally always overestimate the calculated moment values. With the possibility of increasing the active length, the segmented structure enables the compensation of the torque to the expected value and the preparation of a universal MG structure for a whole range of types of booms of various sizes. In summary, introducing magnetic gear (MG) systems to assist the movement of telescopic booms of camera cranes represents a significant advancement in film and television production equipment. MGs offer an attractive solution to increase safety and ergonomics in this industry niche. This innovation promises to improve the performance and safety of camera crane systems, setting the stage for further advances in film and television production technology.

## REFERENCES

- [1] B. Yan, X. Li, X. Wang, and Y. Yang, "A review on the field-modulated magnetic gears: Development status, potential applications, and existent challenges," *IET Electr. Power Appl.*, vol. 18, no. 1, pp. 1–19, 2024, doi: [10.1049/elp2.12365](https://doi.org/10.1049/elp2.12365).
- [2] G. Ruiz-Ponce, M.A. Arjona, C. Hernandez, and R. Escarela-Perez, "A review of magnetic gear technologies used in mechanical power transmission," *Energies*, vol. 16, p. 1721, 2023, doi: [10.3390/EN16041721](https://doi.org/10.3390/EN16041721).
- [3] K. Atallah and D. Howe, "A novel high-performance magnetic gear," *IEEE Trans. Magn.*, vol. 37, pp. 2844–2846, 2001, doi: [10.1109/20.951324](https://doi.org/10.1109/20.951324).
- [4] J. Ribrant and L.M. Bertling, "Survey of failures in wind power systems with focus on Swedish wind power plants during 1997–2005," *IEEE Trans. Energy Convers.*, vol. 22, no. 1, pp. 167–173, 2007, doi: [10.1109/TEC.2006.889614](https://doi.org/10.1109/TEC.2006.889614).
- [5] L. Jing, T. Zhang, Y. Gao, R. Qu, Y. Huang, and T. Ben, "A novel hts modulated coaxial magnetic gear with eccentric structure and halbach arrays," *IEEE Trans. Appl. Supercond.*, vol. 29, no. 5, pp. 1–5, 2019, doi: [10.1109/TASC.2019.2892152](https://doi.org/10.1109/TASC.2019.2892152).
- [6] M. Johnson, A. Shapoury, P. Boghrat, M. Post, and H.A. Toliyat, "Analysis and development of an axial flux magnetic gear," in *2014 IEEE Energy Conversion Congress and Exposition (ECCE)*, 2014, pp. 5893–5900, doi: [10.1109/ECCE.2014.6954210](https://doi.org/10.1109/ECCE.2014.6954210).
- [7] H.Y. Wong, H. Baninajar, B.W. Dechant, P. Southwick, and J.Z. Bird, "Experimentally testing a halbach rotor coaxial magnetic gear with 279 nm/l torque density," *IEEE Trans. Energy Convers.*, vol. 38, no. 1, pp. 507–518, 2023, doi: [10.1109/TEC.2022.3208320](https://doi.org/10.1109/TEC.2022.3208320).
- [8] A. Penzkofer and K. Atallah, "Magnetic gears for high torque applications," *IEEE Trans. Magn.*, vol. 50, no. 11, pp. 1–4, 2014, doi: [10.1109/TMAG.2014.2328093](https://doi.org/10.1109/TMAG.2014.2328093).
- [9] P.O. Rasmussen, T.V. Frandsen, K.K. Jensen, and K. Jessen, "Experimental evaluation of a motor-integrated permanent-magnet gear," *IEEE Trans. Ind. Appl.*, vol. 49, no. 2, pp. 850–859, 2013, doi: [10.1109/TIA.2013.2242423](https://doi.org/10.1109/TIA.2013.2242423).
- [10] L. Jing, W. Liu, W. Tang, and R. Qu, "Design and optimization of coaxial magnetic gear with double-layer pms and spoke structure for tidal power generation," *IEEE-ASME Trans. Mechatron.*, vol. 28, no. 6, pp. 3263–3271, 2023, doi: [10.1109/TMECH.2023.3261987](https://doi.org/10.1109/TMECH.2023.3261987).
- [11] Z.A. Cameron, T.T. Tallerico, and J.J. Scheidler, "Lessons learned in fabrication of a high-specific-torque concentric magnetic gear," in *Vertical Flight Society Annual Forum and Technology Display*, 2019, doi: [10.4050/f-0075-2019-14682](https://doi.org/10.4050/f-0075-2019-14682).
- [12] M. Kowol, J. Kołodziej, and M. Łukaniszyn, "Optimization results of a permanent magnetic (pm) gear (Optymalizacja pasywnej przekładni magnetycznej)," *Prz. Elektrotechniczny*, vol. 93, pp. 78–82, 2017, doi: [10.15199/48.2017.02.19](https://doi.org/10.15199/48.2017.02.19).
- [13] M. Kowol, J. Kołodziej, M. Jagiela, and M. Łukaniszyn, "Impact of modulator designs and materials on efficiency and losses in radial passive magnetic gear," *IEEE Trans. Energy Convers.*, vol. 34, pp. 147–154, 2019, doi: [10.1109/TEC.2018.2862462](https://doi.org/10.1109/TEC.2018.2862462).
- [14] G. Jungmayr, J. Loeffler, B. Winter, F. Jeske, and W. Amrhein, "Magnetic gear: Radial force, cogging torque, skewing, and optimization," *IEEE Trans. Ind. Appl.*, vol. 52, no. 5, pp. 3822–3830, 2016, doi: [10.1109/TIA.2016.2571267](https://doi.org/10.1109/TIA.2016.2571267).
- [15] C.J. Agenbach, D.N.J. Els, R.J. Wang, and S. Gerber, "Force and vibration analysis of magnetic gears," in *2018 XIII International Conference on Electrical Machines (ICEM)*, 2018, pp. 752–758, doi: [10.1109/ICELMACH.2018.8506690](https://doi.org/10.1109/ICELMACH.2018.8506690).
- [16] M. Kowol, J. Kołodziej, R. Gabor, M. Łukaniszyn, and M. Jagiela, "On-load characteristics of local and global forces in co-axial magnetic gear with reference to additively manufactured parts of modulator," *Energies*, vol. 13, p. 3169, 2020, doi: [10.3390/en13123169](https://doi.org/10.3390/en13123169).
- [17] G. Jungmayr, J. Loeffler, B. Winter, F. Jeske, and W. Amrhein, "Magnetic gear: Radial force, cogging torque, skewing and optimization," in *2015 IEEE Energy Conversion Congress and Exposition (ECCE)*, 2015, pp. 898–905, doi: [10.1109/ECCE.2015.7309783](https://doi.org/10.1109/ECCE.2015.7309783).